



## OPEN ACCESS

## EDITED BY

Shuyang Liu,  
China University of Petroleum (East  
China), China

## REVIEWED BY

Hao Chen,  
Xi'an University of Architecture and  
Technology, China  
Muhammad Imran Rashid,  
University of Engineering and  
Technology, Lahore, Pakistan

## \*CORRESPONDENCE

Yihang Zhang,  
Luckzhangyh@foxmail.com

## SPECIALTY SECTION

This article was submitted to Carbon  
Capture, Utilization and Storage,  
a section of the journal  
Frontiers in Energy Research

RECEIVED 18 August 2022

ACCEPTED 26 September 2022

PUBLISHED 16 January 2023

## CITATION

Zhang Y and Huang Y (2023), Study on  
multicomponent composite anti-  
corrosion cement slurry system suitable  
for ultra-high temperature acid  
gas wells.

*Front. Energy Res.* 10:1022446.  
doi: 10.3389/fenrg.2022.1022446

## COPYRIGHT

© 2023 Zhang and Huang. This is an  
open-access article distributed under  
the terms of the [Creative Commons  
Attribution License \(CC BY\)](https://creativecommons.org/licenses/by/4.0/). The use,  
distribution or reproduction in other  
forums is permitted, provided the  
original author(s) and the copyright  
owner(s) are credited and that the  
original publication in this journal is  
cited, in accordance with accepted  
academic practice. No use, distribution  
or reproduction is permitted which does  
not comply with these terms.

# Study on multicomponent composite anti-corrosion cement slurry system suitable for ultra-high temperature acid gas wells

Yihang Zhang\* and Yang Huang

School of Civil Engineering, Chongqing Industry Polytechnic College, Chongqing, China

In the field of oil cementing, corrosion has always been a major problem that perplexes researchers. In the past, the research mainly focused on solving the corrosion problem of cement stone with temperature below 150°C, and there was a lack of corrosion research cases for ultra-high temperature. In addition, the gas channeling problem in the cementing of ultra-high temperature acid gas wells cannot be ignored, which further increases the difficulty in the design of anti-corrosion cement slurry system. Therefore, from the perspective of anti-corrosion, gas channeling and high temperature resistance, this paper uses hydroxyapatite blast furnace slag and functional temperature resistant and anti-corrosion composite emulsion as anti-corrosion additives to build a multi-component composite ultra-high temperature anti-corrosion cement slurry system with good engineering performance and a density range of 1.9 g/cm<sup>3</sup>-2.4 g/cm<sup>3</sup>, and analyzes its microstructure and phase composition. The corrosion inhibition mechanism of multicomponent composite cement paste was discussed.

## KEYWORDS

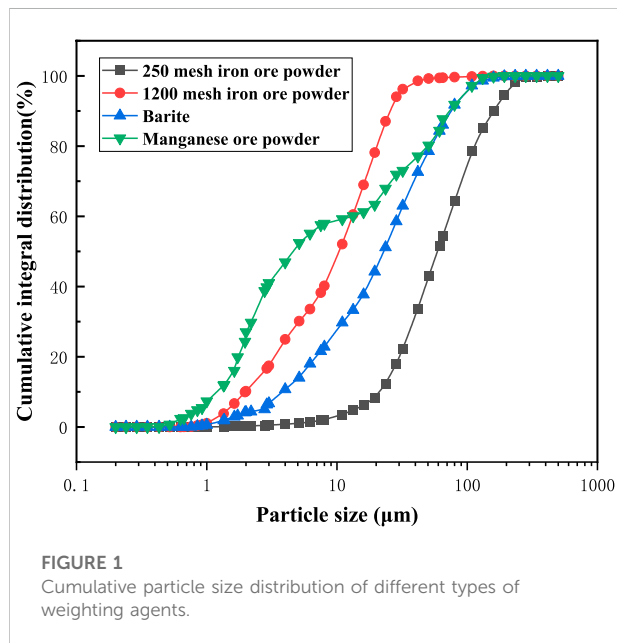
composite emulsion, ultra high temperature, CO<sub>2</sub> corrosion, oil well cement, gas channeling

## 1 Introduction

In the cementing operation of ultra-high temperature acid gas wells, the cementing cement sheath is usually affected by acid corrosion, resulting in the obstruction of oil and gas production (Erik et al., 1990; Wang et al., 2012; Xue et al., 2013). On the one hand, corrosive media will damage the cement between cement sheath and formation, resulting in inter layer channeling; On the other hand, the corrosive medium will continue to migrate inward along with the seepage channel, and directly act on the casing and tubing, causing perforation or even scrapping of the whole well, which will cause huge economic losses and a series of safety accidents (Liu et al., 2001; Rogers et al., 2004). Therefore, on the premise of ensuring that the basic performance of oil well cement stone meets the requirements of conventional cementing operation, it is the key to improve the quality of

TABLE 1 Chemical composition of Jiahua grade G oil well cement.

Component	SiO <sub>2</sub>	MgO	K <sub>2</sub> O	Na <sub>2</sub> O	Fe <sub>2</sub> O <sub>3</sub>	CaO	Al <sub>2</sub> O <sub>3</sub>	Others
Content (%)	20.52	1.36	0.43	0.51	4.78	63.42	2.61	6.37



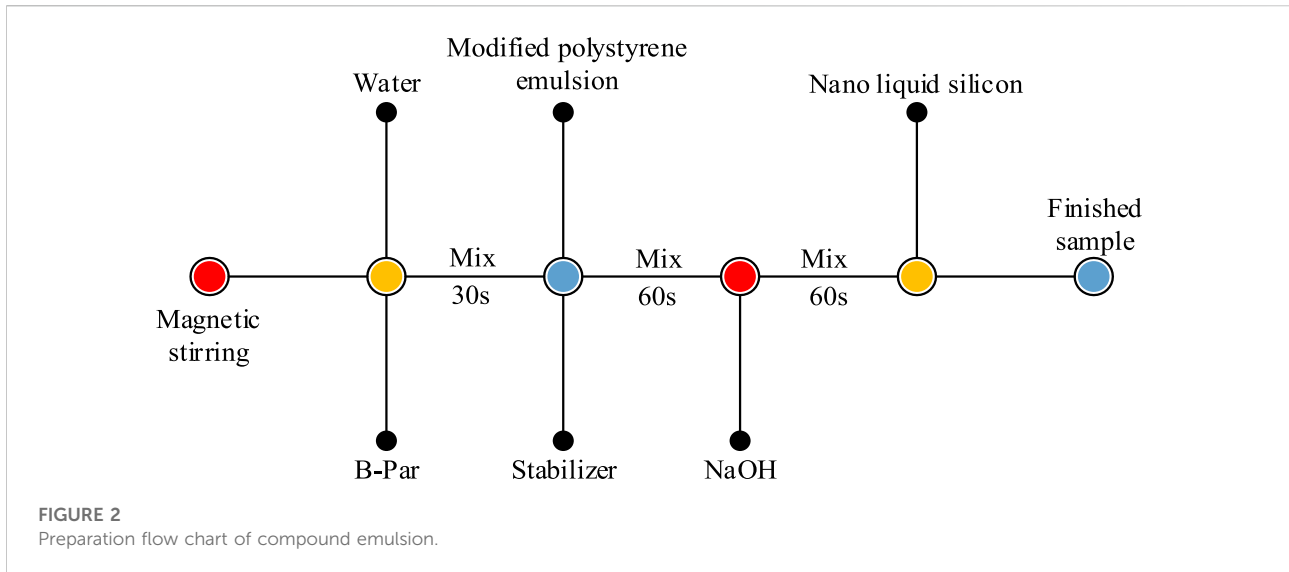
such complex cementing to carry out research on the corrosion and gas channeling prevention of cement. At the same time, it is also the premise to ensure the long-term stable production of ultra-high temperature acid gas wells (Moore et al., 2012).

Scientific researchers have done a lot of research to improve the corrosion resistance of cementing cement stone. Yuan et al. (2018) reduced the original permeability and average pore diameter of cement stone by 3.35 times and 35.38% respectively by taking advantage of the film formation and filling effect of nano silica latex (NL). In addition, NL reacts with Ca(OH)<sub>2</sub> to form tobermorite with low Ca/Si ratio, which reduces the pH value of cement. Rooby et al. (2021) studied the influence of nano CaCO<sub>3</sub> (CFC), nano SiO<sub>2</sub>(CFS) and nano ZrO<sub>2</sub>(CFZ) doping on the corrosion performance of fly ash (CF)

cement paste, and found that the nano materials can inhibit the cracking of cement paste and significantly enhance the corrosion resistance. Krivenko et al. (2020) modified soluble sodium silicate (SSS) with surfactant and Na<sub>3</sub>PO<sub>4</sub>, and then explored its influence on slag based cement. The results show that the matrix compactness of slag based cement stone can be significantly improved by using modified SSS, and the mechanical properties and corrosion resistance can be enhanced. Zhang et al. (2020) prepared soap free emulsion (PSAC) by soap free emulsion polymerization with sodium styrene sulfonate (SSS) and nano-SiO<sub>2</sub> as emulsifiers, and evaluated the carbonization performance of PSAC cement under 90°C and 3 Mpa CO<sub>2</sub>. It is found that PSAC has a typical core-shell structure and good heat resistance. After 60 days of corrosion, the corrosion depth of PSAC cement stone is only 2.16 mm, the permeability is 0.0018 mD, and the compressive strength decreases by 6.65%. Xu et al. (2018) constructed a composite anti-corrosion additive (CRA) composed of amorphous nano silica, latex and resin, and studied the corrosion performance of CRA cement stone at 150°C. It is found that the original permeability of CRA cement paste is reduced, the CH phase in the cement paste is reduced, the hydration product Ca/Si is reduced, and the corrosion resistance of the cement paste is enhanced. Zuo et al. (2020) explored the influence of epoxy resin emulsion combined with metakaolin (MK) on the corrosion performance of cement paste, and found that after adding MK, the water absorption and chloride ion diffusion coefficient of epoxy resin emulsion cement paste were significantly reduced, the maximum decrease of chloride ion diffusion coefficient of 1250 mesh MK was 73.1%. However, there are still many problems with the above-mentioned anti-corrosion additives. The performance of conventional polymer and resin materials deteriorates obviously under high and ultra-high temperature conditions, and has a great impact on the thickening process of cement slurry; The acid resistant particles have good slurry fluidity when the particle size

TABLE 2 Particle size distribution of different types of weighting agents.

Weighting agents	D10/μm	D25/μm	D50/μm	D75/μm	D90/μm	D97/μm	D (3,2)/μm	D (4,3)/μm
Manganese ore powder	1.23	1.96	4.38	35.8	77.0	111.6	2.94	23.9
Barite	3.84	8.86	22.9	45.1	75.0	105.9	32.2	9.39
250 mesh iron ore powder	21.5	34.4	59.0	99.8	159.7	216.3	75.2	36.4
1200 mesh iron ore powder	1.98	4.01	10.5	18.3	25.3	33.9	12.7	5.23



is large, but the settling stability is poor. When the particle size is small, the slurry fluidity will be reduced and the pumping difficulty will be increased; Most inorganic mineral powders have good compatibility with cement paste, but it will greatly reduce the early compressive strength of cement paste.

In view of the above problems, from the perspective of anti-corrosion, channeling prevention and high temperature resistance, this paper uses HA, BF<sub>3</sub> and functional temperature resistant and anti-corrosion composite emulsion as anti-corrosion additives to build a multi-component composite ultra-high temperature anti-corrosion cement slurry system with a density range of 1.9 g/cm<sup>3</sup>-2.4 g/cm<sup>3</sup> and good engineering performance, and analyzes its microstructure and phase composition, and discusses the corrosion inhibition mechanism of multi-component composite cement paste. The research results of this paper provide scientific basis for the research of ultra-high temperature anti-corrosion cement slurry

system and its application in cementing engineering, and have extremely important significance for improving the temperature resistance and anti-corrosion performance of cementing cement paste and realizing safe production.

## 2 Materials and methods

### 2.1 Experimental materials

Jiahua Grade G oil well cement, the raw material was purchased from Sichuan Jiahua Enterprise (Group) Co., Ltd., the specific chemical composition is shown in Table 1, Nano liquid silicon, purchased from Wuhu Jikang New Material Technology Co., Ltd., its basic parameters are: particle size 10–20 nm, purity >99.9%, molecular weight 60.08, SiO<sub>2</sub> content 20 ± 1%, pH = 9–10, viscosity <500 cP, Iron ore

TABLE 3 Composition of cement slurry formula.

Density	Cement	Silica fume	Dispersant	Filterate reduce	Composite emulsion	HA	Iron ore powder	Manganese ore powder	BFs	Redorder	Expansive agent	Water
1.9	100	35	3.9	4.9	6	5	0	0	10	2.5	0	66
2.0	100	35	3.9	4.9	6	5	23	5	10	2.5	1	66
2.1	100	35	4.3	4.9	6	5	36.6	8	10	2.5	1	67
2.2	100	35	4.5	4.9	6	5	60	13	10	2.5	1	68
2.3	100	35	5	4.9	6	5	96.6	20	10	2.5	1	70
2.4	100	35	5.4	4.9	6	5	115	25	10	2.5	1	71

Unit: density—g/cm<sup>3</sup>; formula dosage—%.

TABLE 4 Evaluation criteria for gas channeling prevention performance of SPN.

SPN	<3	3–6	>6
Anti-gas channeling performance	Well	Medium	Poor

powder ( $\rho = 4.89 \text{ g/cm}^3$ ), purchased from Runhui Mineral Products Processing Plant in Lingshou County, Barite, purchased from Lingshou County Maozhuo Building Materials Co., Ltd. Manganese ore powder ( $\rho = 4.75 \text{ g/cm}^3$ ), purchased from Hunan Daji Manganese Industry Co., Ltd. The particle size distribution of the weighting agent is shown in Figure 1 and Table 2. Blast furnace slag (BFs) and fly ash (FA) were purchased from Lingshou County Yiran Mineral Products Processing Plant, Hydroxyapatite, the raw material was purchased from Xi'an Jinheng Chemical Co., Ltd. Compound silica fume, B-Par polymer (the main component is polyethyleneimine), high temperature retarder H66L, modified polystyrene latex (GR), dispersants CF44L and CF40L, fluid loss reducer CG80L, and defoamer X66L are all from Jiahua Technology Co., Ltd. The functional temperature-resistant composite emulsion is self-made in the laboratory. Its preparation process and component state are shown in Figure 2 and Figure 3.

It can be seen from Table 2 that the order of D50 median particle size distribution of different weighting agents is: D (250 iron ore > barite > 1200 iron ore powder > manganese ore powder). After a reasonable ratio, the compound of manganese ore powder and 250 mesh iron ore powder (12:55) was determined as the main weighting agent of the high-density cement slurry system.

The compound emulsion preparation process is shown in Figure 2: In a high-speed stirring environment, add 9% B-Par polymer solution to an appropriate amount of laboratory water, and after mixing for 1 min, add 7% modified polystyrene on this basis the latex and surfactant mixture, continue to stir at high speed for 60 s. Subsequently, 6% nano-liquid silicon and 0.2% NaOH particles were mixed into the mixed solution, and mixed for 60 s to obtain a composite emulsion.

In the principle of solution mixing, the liquid phase admixture is mixed first, and then the solid phase admixture is mixed. On the one hand, the liquid-phase admixture will increase the viscosity of the solution, and the solid-phase particle mixing on this basis will help to improve the suspension and dispersion effect of the solid-phase particles. On the other hand, the liquid-phase admixture has a certain dilution effect, which can effectively reduce the initial viscosity of b-par polymer and avoid uneven mixing of emulsion. The composition and final state of the solution in the composite emulsion are shown in Figure 3.

The constructed functional composite emulsion system is: 6% nano-liquid silicon +6% modified temperature-resistant latex

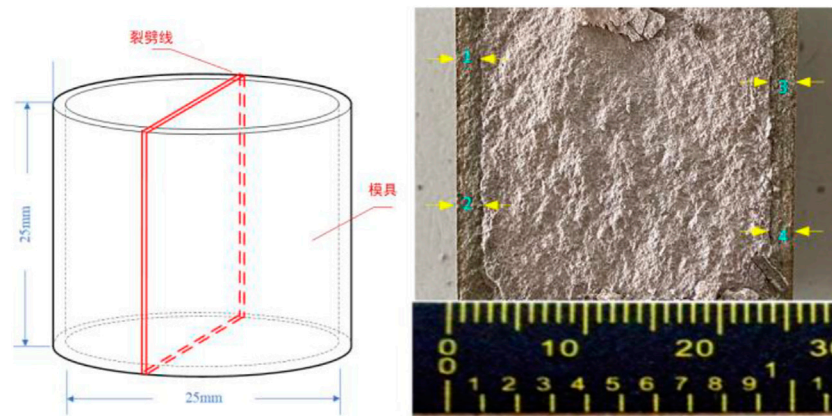


**FIGURE 4**  
Determination method of corrosion depth of cement paste (Zhang et al., 2022).

+1% stabilizer +9% B-Par polymer (the main component is polyethyleneimine) + 0.2% NaOH solid phase particles. The characteristics of the emulsion are mainly reflected in: based on the modified temperature-resistant latex, combined with high-temperature (>180°C) B-Par polymer can effectively reduce the primary pores inside the cement stone, thereby significantly improving the cement stone matrix density, and the emulsion can effectively reduce the water loss of the cement slurry at high temperature, and avoid the gas channeling problem caused by the water loss of the cement slurry. In addition, the alkaline particles in the composite emulsion can stimulate the inorganic mineral powder to form a crystalline phase, thereby improving the matrix compactness of the cement stone.

## 2.2 Experimental formula

Through the combination design and addition amount optimization of anti-corrosion admixtures, a multi-component composite anti-corrosion cement slurry system with good performance is constructed. However, it is necessary to further study the engineering performance of the multi-component composite anti-corrosion cement slurry system under different densities in combination with the actual working conditions. Therefore, based on the BFs-HA-composite emulsion-based cement slurry system, the experimental formula was constructed as shown in Table 3:

## 2.3 Experimental process and method

### 2.3.1 General performance

According to the petroleum industry standard GB/T 19,139-2012 test method for oil well cement, the rheological

parameters of the cement slurry under different rotating speeds are measured. The filtrate volume of the cement slurry within 30 min is measured with a high temperature and high-pressure water loss meter (93°C, 6.9 MPa), and the high-temperature and high-pressure Thickener (220 °C × 90 MPa), and the compressive strength of cement paste was tested by TH-8100S universal testing machine. The sample size was 50.8 × 50.8 × 50.8 mm.

### 2.3.2 Gas channeling performance

Before evaluating the corrosion performance of anti-corrosion materials, it is necessary to preliminarily evaluate the anti-channeling ability of different anti-corrosion materials. To accurately judge the anti-channeling ability of the ultra-high temperature cement slurry system, the performance coefficient method combined with the ultrasonic static gel strength analyzer was used. The cement slurry performance coefficient method (*SPN*) is the most widely used evaluation method at home and abroad (Sutton et al., 1984; Kwatia et al., 2019; Ramadan et al., 2019). The formula is as follows:

$$SPN = \frac{B(\sqrt{t_{100}Bc} - \sqrt{t_{30}Bc})}{\sqrt{30}} \quad (1)$$

Where, *SPN* is the coefficient of performance of cement slurry, dimensionless, *B* is the water loss API of cement slurry 6.9 MPa, 30 min/ml,  $t_{100}Bc$  and  $t_{30}Bc$  are the time when the consistency of the cement slurry thickening experiment reaches 30 *Bc* and 100 *Bc* respectively, min.

The advantages of this method are as follows: to a certain extent, it reflects the relationship between the water loss, strength development and gas intrusion process of the cement slurry, the experimental parameters are easy to obtain, and the calculation method is simple. The specific evaluation criteria are shown in Table 4.

TABLE 5 Rheological properties of multicomponent composite anti-corrosion cement slurry system under different densities.

Cement slurry density	Rheological properties of cement slurry at 93°C					
/G/cm <sup>3</sup>	φ600	φ300	φ200	φ100	φ6	φ3
1.9	—	284	202	121	11	8
2.0	—	272	199	106	14	12
2.1	—	278	201	110	15	13
2.2	—	262	187	95	13	10
2.3	—	258	176	88	14	12
2.4	—	260	199	99	16	14

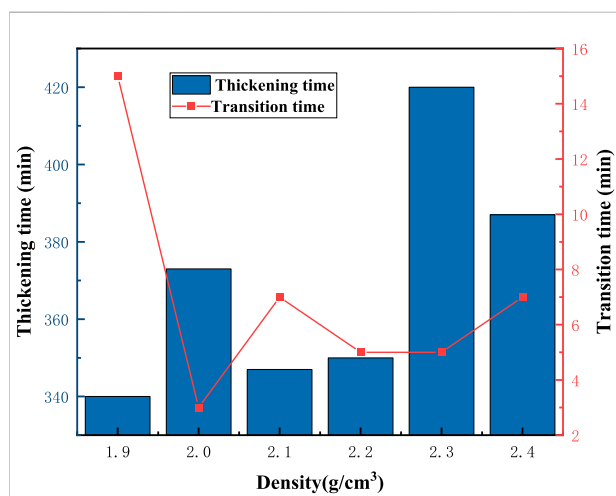


FIGURE 5 Thickening properties of multicomponent composite anti-corrosion cement slurry system under different densities.

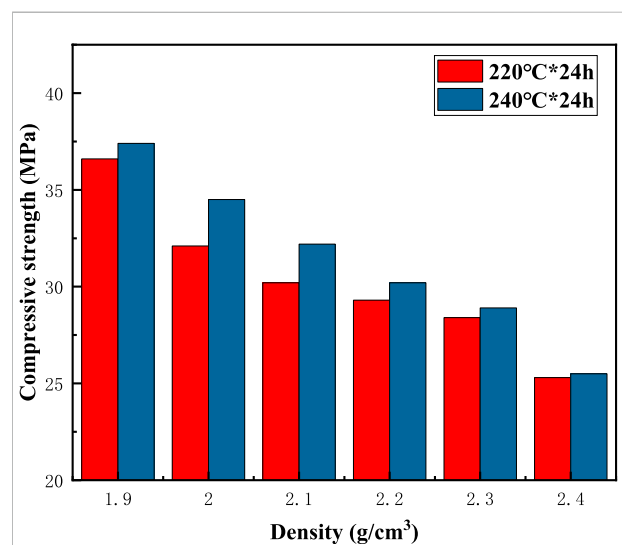


FIGURE 6 Mechanical properties of multicomponent composite anti-corrosion cement slurry system under different densities.

In addition, the ultrasonic static gel strength analyzer was used to evaluate the anti-channeling performance of the multicomponent composite ultra-high temperature anti-corrosion cement slurry system. The experimental temperature was controlled at 200°C, and the pressure value setting was consistent with the thickening test.

### 2.3.3 Corrosion performance

#### 1) Corrosion depth

The corrosion depth is the thickness of the carbonized layer after the cement stone is corroded. Correspondingly, the curing period of the cement stone sample in the corrosive environment is the corrosion age, and the curing age refers to the curing time of the cement stone in the wet environment (or the wet corrosive environment). Due to the high

temperature of the corrosion experiment in this paper, the alkaline substance in the cement stone is basically consumed, and the color developing effect of the acid-base indicator has completely disappeared. However, the corrosion interface of the cement stone under high temperature is relatively clear, so it is mainly identified by naked eyes and observed with the aid of a microscope. Through the midline splitting of the cement stone under the constant corrosion age and the selection of four corrosion thicknesses on the side of the corrosion layer, Then, the average value (as shown in Figure 4) is obtained to obtain the corrosion depth value.

#### 2) Compressive strength

For the compressive strength test method of the corrosion test, the compressive strength of the cement stone before and

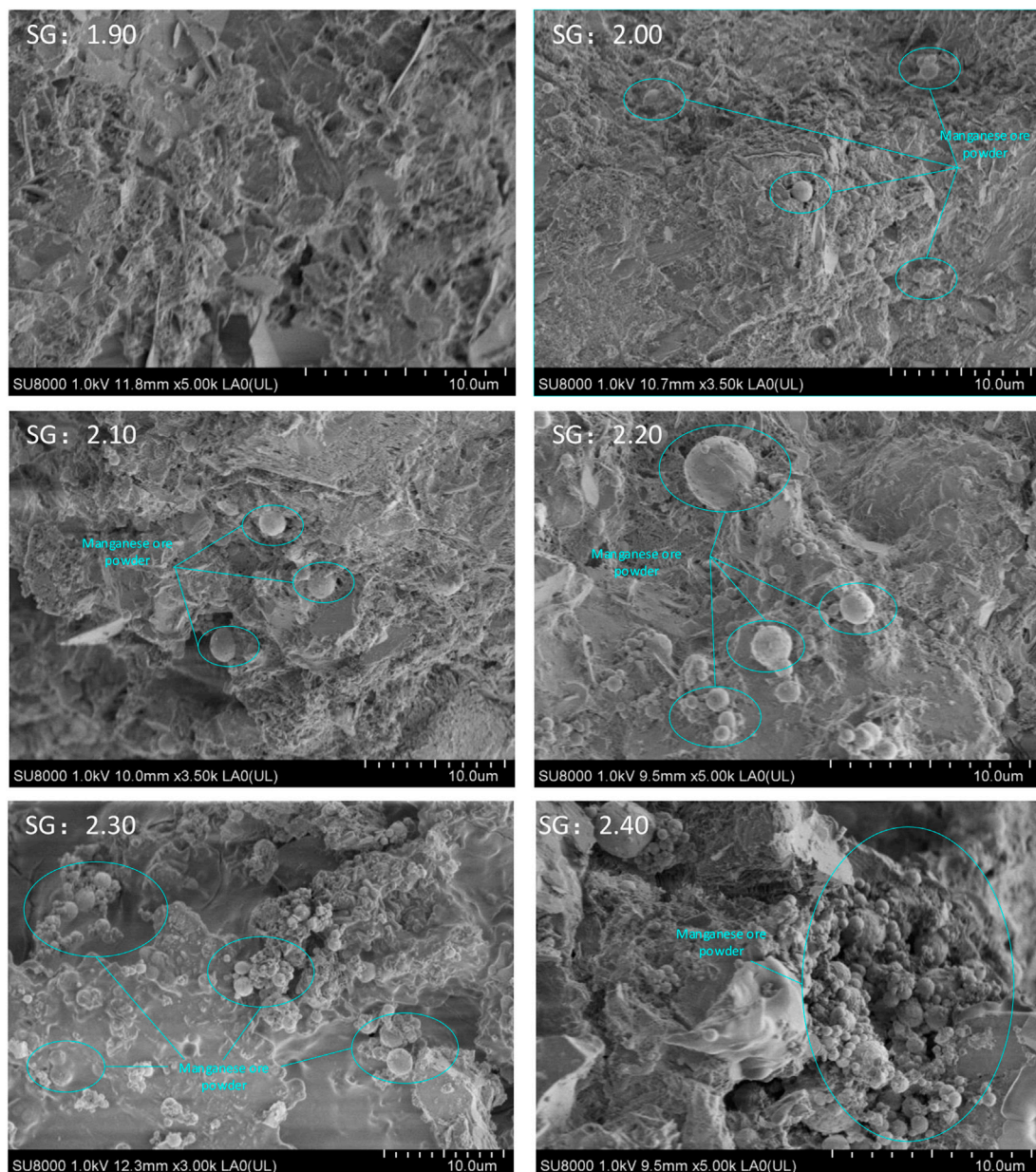


**FIGURE 7**  
Microstructure of multicomponent composite anti-corrosion cement slurry system under different densities.

after corrosion was measured according to the national standard GB//T199139-2012 “Cementing Stone Test Method”, and the compressive strength decay rate was calculated.

The formula for calculating the compressive strength is:

$$P = \frac{40F}{\pi d^2} \tag{2}$$

Where,  $P$  is compressive strength (MPa),  $F$  is press reading (kN),  $d$  is specimen diameter (cm).

By measuring the compressive strength of the cement stone before and after corrosion, the decay rate of the compressive strength of the cement stone is calculated. The calculation formula is:

$$\alpha = \frac{P - P_i}{P} \tag{3}$$

Where,  $\alpha$  is the compressive strength decay value (%),  $P$  is the initial compressive strength (MPa), and  $P_i$  is the compressive strength after the  $i$  th day (MPa).

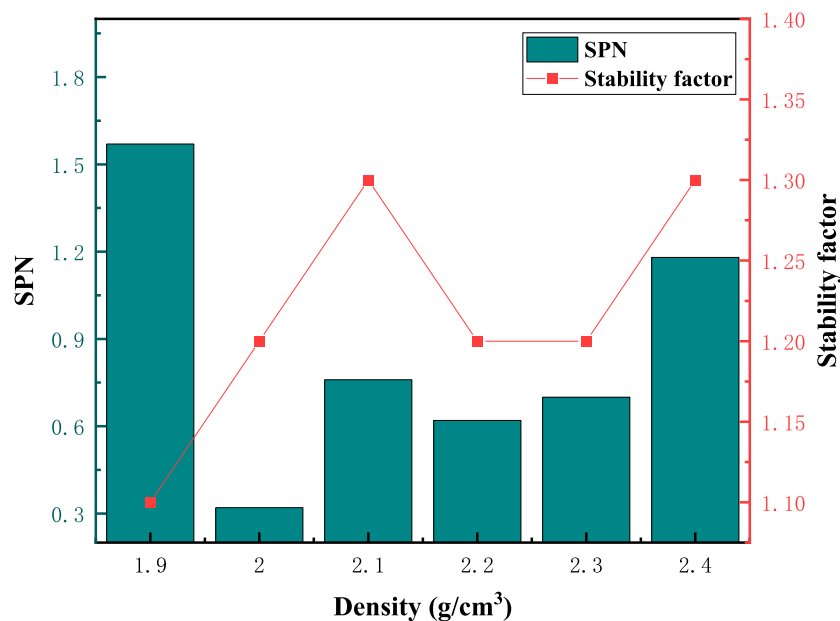


FIGURE 8

Channeling resistance of multicomponent composite anti-corrosion cement slurry system under different densities.

### 3) Permeability

Permeability reflects the ability of cement stone matrix to transmit fluid, and determines the erosion difficulty and erosion area of corrosive medium to cement stone. As one of the important parameters to judge the change of cement stone hole, it plays an important role in evaluating the corrosion degree of cement stone. According to the American Petroleum Institute standard (API RP-40), HKY-200 pulse decay gas permeability tester is used to measure the permeability of cement stone samples. The equipment measurement range is 0.00001–10 mD, pore pressure is 6.9 MPa, and the maximum confining pressure is 69 MPa.

## 2.4 Testing of microstructure of cement paste

### 1) SEM

The cement profile was sampled and analyzed by Hitachi S-4800 field emission scanning electron microscope (SEM). The acceleration voltage of electron beam was 15 kV.

### 2) XRD diffraction analysis

The composition of cement before and after corrosion under different corrosion conditions is analyzed by BRUKER

D8 ADVANCE X-ray diffractometer. The maximum tube voltage of the equipment is 60 kV, the maximum tube current is 80 mA, the scanning speed is 2°/min, and the scanning range is 5°–80°.

## 3 Results and discussion

### 3.1 Rheological properties

In engineering application, the fluidity of cement slurry directly determines the workability of slurry preparation and the difficulty of pressurized pumping. To ensure the engineering performance of cement slurry system under different densities, based on the identified admixtures, the rheological properties of BFs-HA-composite emulsion system with different densities were carried out indoors. The specific experimental results are shown in Table 5.

It can be seen from Table 5 that under different density cement slurry formulations, the dispersant can be adjusted slightly to ensure that  $\phi$  300 is shown. Meanwhile, with the increase of density, the fluidity of cement slurry is improved. On the one hand, due to the increase of dispersant dosage, and on the other hand, due to the lubrication effect of spherical manganese ore powder, the friction resistance between particles is effectively reduced.



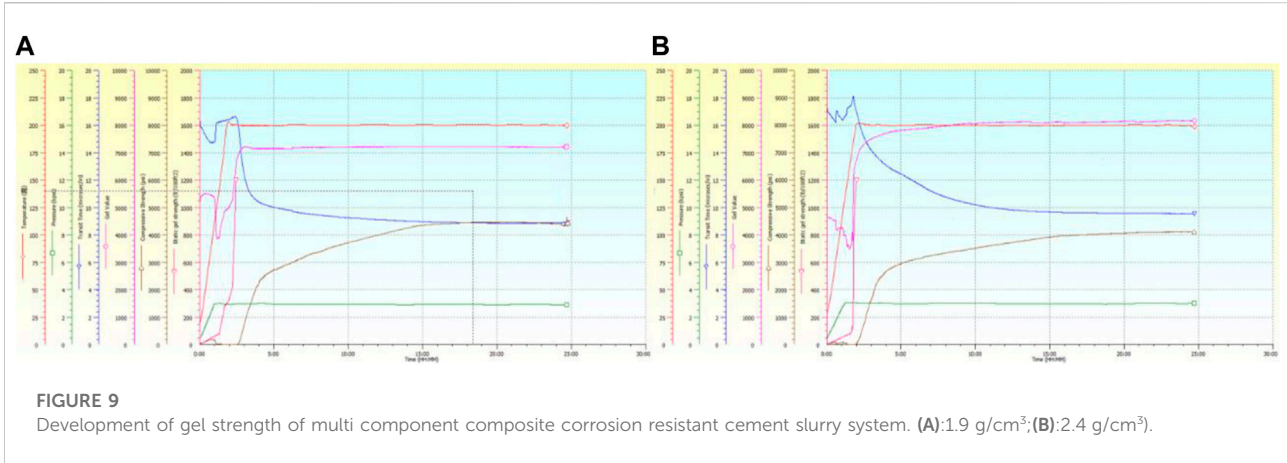


FIGURE 9 Development of gel strength of multi component composite corrosion resistant cement slurry system. (A):1.9 g/cm<sup>3</sup>; (B):2.4 g/cm<sup>3</sup>.

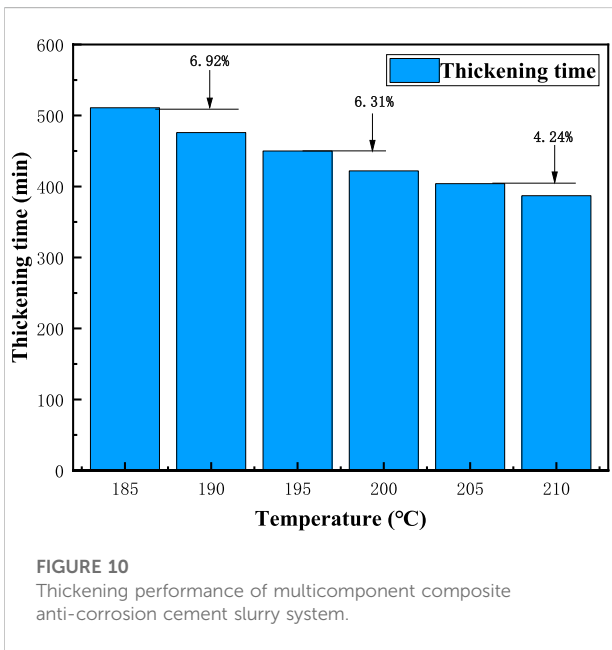


FIGURE 10 Thickening performance of multicomponent composite anti-corrosion cement slurry system.

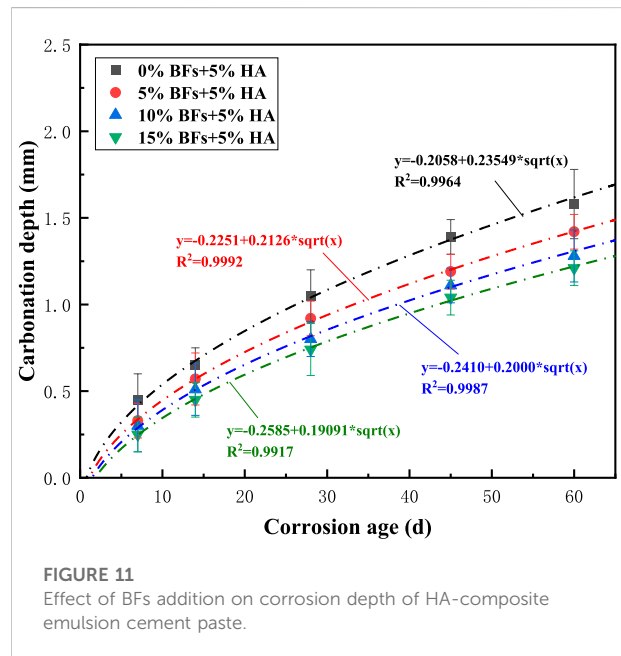


FIGURE 11 Effect of BFs addition on corrosion depth of HA-composite emulsion cement paste.

### 3.2 Thickening properties

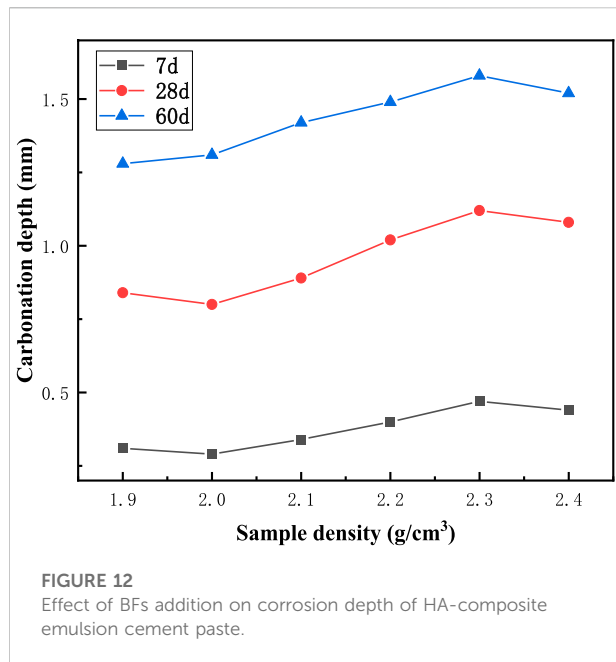
The thickening performance of cement slurry is very important to ensure that the cement slurry can be effectively sealed before the formation of gas channeling channel at the specified time and at the specified layer. In ultra-high temperature acid gas wells, the thickening time of cement slurry is usually required to be more than 5 h and the conversion time is less than 30 min. Therefore, this paper evaluates the thickening time and thickening transition time of cement slurry systems with different densities at 220°C, and the experimental results are shown in Figure 5.

It can be seen from Figure 5 that by controlling the dosage of retarder, the thickening time of the cement slurry system can be

stably controlled at more than 300 min, so that it has enough time to pump to the target horizon. In addition, with the increase of the density value of the cement slurry system, the thickening transition time of the cement slurry decreases, which is due to the increase of the weighting agent dosage, which reduces the liquid-solid ratio of the cement slurry and thus shortens the setting time of the hydration products.

### 3.3 Mechanical properties

Since the weighting agent cannot participate in the hydration process of cement slurry, when dispersed and filled in the hydration products, the contact area between cements will



become smaller, thus reducing the mechanical properties of cement paste. To ensure that the multi-component composite anti-corrosion cement stones under different densities have high compressive strength, the mechanical properties of the cement stones cured at 220°C (target temperature) and 240°C (limit temperature) are evaluated respectively. The experimental results are shown in Figure 6.

It can be seen from Figure 6 that the compressive strength of cement paste decreases regularly with the increasing density of cement slurry system. The compressive strength of cement stone at 220°C and 240°C is greater than 20 MPa, which meets the needs of field working conditions, and the compressive strength of cement stone at 240°C is greater than that at 220°C as a whole. The reason is that with the addition of high-dose silica fume, the higher curing temperature accelerates the complete hydration and pozzolanic effect of cement stone (Zhang et al., 2014).

To verify the reasons for the differences in mechanical properties of anti-corrosion cement stones with different densities, profile samples of cement stones with different densities were taken respectively, and their microstructure was observed and analyzed by scanning electron microscope. The observation multiple was 10 μm. The specific evaluation results are shown in Figure 7.

It can be seen from Figure 7 that massive siliceous structure and a large amount of hydrated cement can be seen in the profile of cement stone with density of 1.9 g/cm<sup>3</sup>, with high structural integrity, no obvious crack defects and no weighting agent. With the increase of weighting agent dosage, spherical manganese ore particles can be seen at the section of cement stone. When the density of cement slurry is

2.3–2.4 g/cm<sup>3</sup>, most of the weighting agent particles are agglomerated and stacked, which will cause the weighting agent bulk density in some areas of cement paste to be too high and cannot form an effective cementation structure, so that the compressive strength of cement paste will decrease with the increase of weighting agent proportion.

### 3.4 Anti-channeling performance

As with conventional gas wells, the possibility of cement slurry gas channeling should also be considered in cementing operation of ultra-high temperature gas wells. Therefore, the SPN value and pressure stability coefficient of the multi-component composite anti-corrosion cement slurry system under different densities are calculated respectively. The specific results are shown in Figure 8.

It can be seen from Figure 8 that the SPN value of the anti-corrosion cement slurry system under different densities is all less than 3, and the pressure stability coefficient is greater than 1, which has a good anti-channeling effect. In addition, the ultrasonic static gel strength analyzer was used to evaluate the gel strength development process of different densities of anti-corrosion cement slurry systems. The experimental temperature is 200 °C and the pressure is 21 MPa. The experimental results are shown in Figure 9.

It can be seen from Figure 9 that the conversion time of different densities of anti-corrosion cement slurry systems from 48 to 240 Pa is less than 15 min. Due to the short isolation time and the large change in the gel strength, it can ensure that the cement slurry quickly develops strength after being pumped to the target layer, effectively reducing the possibility of the cement slurry losing weight or gas channeling. In addition, the early strength of anti-corrosion cement stone develops rapidly, and the compressive strength within 12 h can reach more than 20 MPa, and maintain a continuous growth trend with the extension of curing age.

### 3.5 Temperature sensitivity

Based on the high temperature and ultra-high temperature operating environment of the target reservoir, it is also necessary to explore the thickening performance of different densities of anti-corrosion cement slurry systems in high temperature well sections. By expanding the experimental temperature range to 160°C–210°C, and taking the anti-corrosion cement slurry system with a density of 2.4 g/cm<sup>3</sup> as the experimental object, the experimental results are shown in Figure 10.

It can be seen from Figure 10 that the thickening time of the anti-corrosion cement slurry system can be stably controlled above 5 h at different temperatures. With the gradual increase of

TABLE 6 Performance changes of composite emulsion cement paste before and after corrosion under different BFs-HA dosage.

BFs(+HA) %	Compressive strength/MPa					Permeability/mD		
	Before corrosion	Corrosion 14 days	Corrosion 28 days	Corrosion 60 days	Rate of change/%	Before corrosion	After corrosion	Rate of change/%
0	37.6	46	36.7	30.9	-17.9	0.0026	0.00307	18.2
5	35.1	42.8	35.9	29.7	-15.4	0.0026	0.00303	16.4
10	36.6	41.9	38.8	35	-4.4	0.0024	0.00248	3.3
15	38	43.2	44.2	39.2	3.2	0.0023	0.00224	-2.5

TABLE 7 Performance change of high density BFs-HA-composite emulsion cement paste before and after corrosion.

->/G/cm <sup>3</sup>	Permeability/mD×10 <sup>-2</sup>		Rate of change/%	Compressive strength/MPa		Rate of change/%
	Before corrosion	After corrosion		Before corrosion	After corrosion	
1.9	0.24	0.25	+3.30	36.6	35.0	-4.40
2.0	0.24	0.24	-1.70	32.1	31.4	-2.10
2.1	0.26	0.28	+6.30	30.2	27.4	-9.40
2.2	0.27	0.30	+11.8	29.3	25.6	-12.7
2.3	0.39	0.45	+15.1	28.4	23.7	-16.6
2.4	0.35	0.40	+13.2	25.3	23.2	-13.2

temperature, the thickening time of cement slurry is gradually shortened, and the sensitivity coefficient (fluctuation range with temperature change) within the temperature range of 160°C–210°C is within 20%.

### 3.6 Corrosion performance

To accurately understand the corrosion law of the anti-corrosion cement slurry formulation system, the corrosion performance test results in the formulation optimization process are reserved in this section.

#### 3.6.1 Corrosion depth variation relationship

By limiting the amount of HA to 5%, BFs material was introduced into the HA-composite emulsion-based cement slurry system, and the secondary cementation of BFs was used to complement HA. The composite emulsion-based cement stone samples were evaluated for corrosion depth, and the experimental results are shown in Figure 11.

It can be seen from Figure 11 that within the age range of 60 days, the corrosion depth of BFs-HA-composite emulsion-based cement stone shows a regular change with the increase of corrosion and curing age, which is consistent with the development law of corrosion depth of conventional slurry

cement stone. All are in line with the  $y = A + B\sqrt{x}$  fitting relation. With the increase of the BFs addition ratio, the corrosion depth of the cement stone gradually decreases, and the corrosion depth of the cement stone under the addition of 10% and 15% BFs is relatively close. Effective anti-corrosion effect.

Based on the combination design of different anticorrosive materials and the performance evaluation of anticorrosive cement slurry system, BFs-HA-composite emulsion was selected to construct a high-density anticorrosive cement slurry system. In the corrosion performance test, the relationship between the corrosion depth of BFs -HA composite emulsion-based cement paste is shown in Figure 12.

It can be seen from Figure 12 that with the increase of the density of the sample, the corrosion depth of the BFs-HA-composite emulsion-based cement stone gradually increases. When the density of the sample is 2.4 g/cm<sup>3</sup> and the corrosion age is 60 days, the corrosion depth of the sample is increased by 12.6% compared with the conventional density. This is because the weighting agent reduces the filling amount of hydration products and stimulates the relative micropores, which leads to the increase of micropores in the cement stone matrix, thereby increasing the corrosion depth of the BFs-HA-composite emulsion-based cement stone.

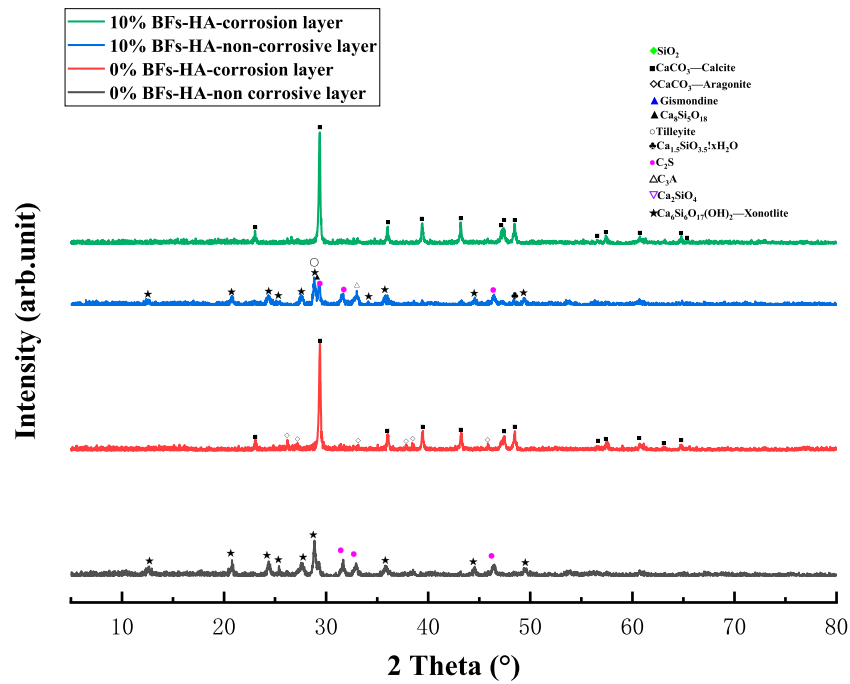


**FIGURE 13**  
XRD spectrum of BFs-HA-composite emulsion-based cement paste corroded inside and outside.

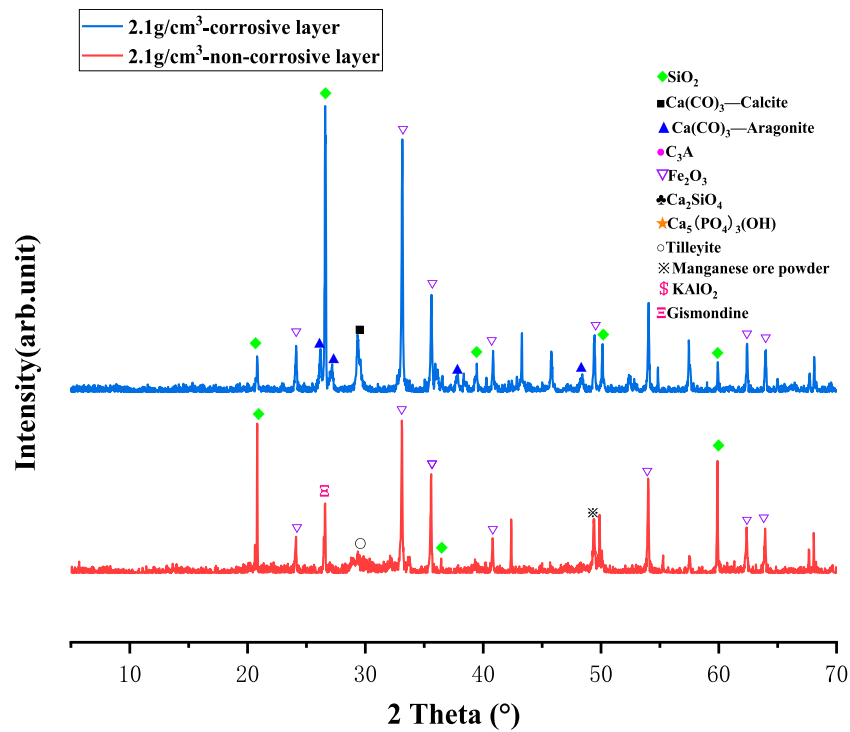


**FIGURE 14**  
XRD spectra of internal and external corrosion of high-density BFs-HA-composite emulsion cement paste.

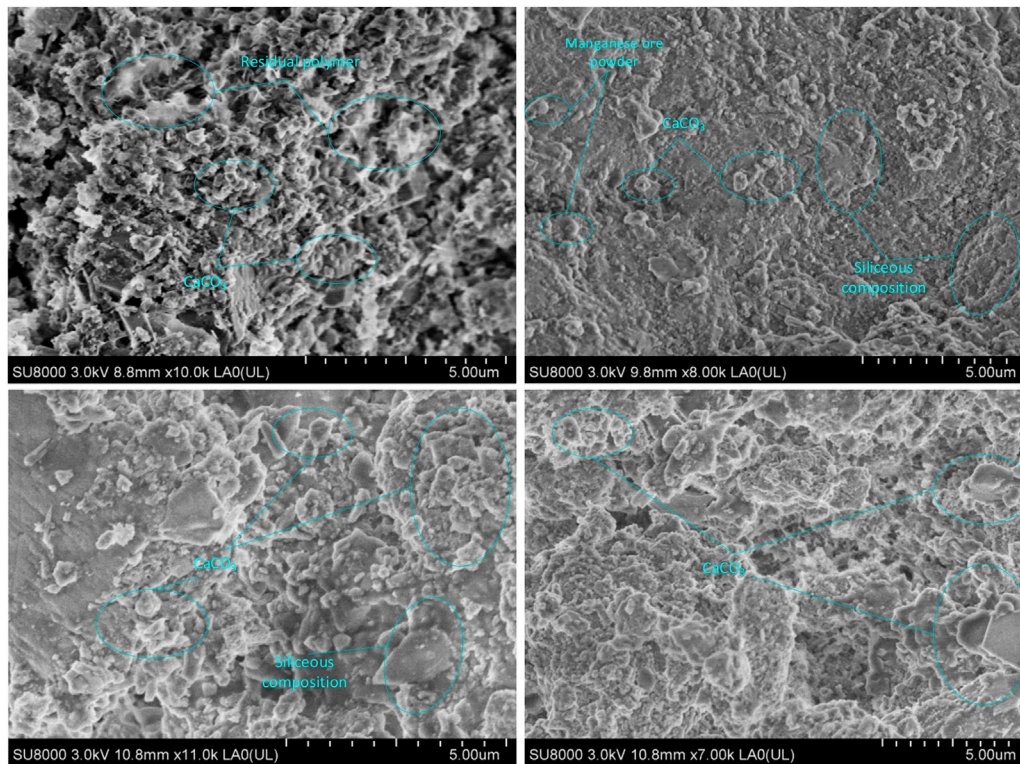


**FIGURE 15**  
Microstructure of corrosion zone of BF-HA-composite emulsion base cement paste.

### 3.6.2 Performance changes of cement stone before and after corrosion

To analyze the performance changes of BF-HA-composite emulsion cement paste before and after corrosion, the compressive strength and permeability of BF-HA-composite emulsion cement at different corrosion ages were studied. The experimental results are shown in Table 6.

It can be seen from Table 6 that with the increasing of BF dosage, the initial compressive strength of BF-HA composite emulsion cement stone decreases first and then increases, while the compressive strength change rate and permeability change rate after 60 days of corrosion gradually decrease. When the BF dosage is 10% and 15% respectively, the compressive strength of BF-HA composite emulsion cement stone at 60 days fluctuates within  $\pm 4.5\%$  compared with that before corrosion, and the permeability fluctuates within  $\pm 3.5\%$  compared with that before corrosion, this shows that in BF-HA composite emulsion cement paste, when BF dosage is 10% or more, relatively stable corrosion performance can be obtained.

The performance of BF-HA composite emulsion with different densities before and after corrosion is evaluated, and the concrete results are shown in Table 7.

From Table 7, it is known that with the increase of the density of samples, the permeability change rate of BF-HA-composite

emulsion cement emulsion increases gradually, and the compressive strength decreases. When the sample density is  $2.4 \text{ g/cm}^3$  and the corrosion age is 60 days, the increase of permeability and the change rate of compressive strength are increased by 10.8% and 9%. This is because the weighting agent cannot participate in the hydration reaction in the cement slurry system. In the action mode, it is mainly suspended in the cement slurry in the form of micro filler, while the use of weighting agent instead of hydrated particles in the same space indirectly reduces the proportion of hydrated particles, resulting in the decrease of cement strength.

### 3.6.3 Phase analysis before and after corrosion

To explore the main reasons for a series of changes of BF-HA-composite emulsion-based cement stone under ultra-high temperature wet-phase corrosion conditions, the corrosion age of 28 days, 0% and 10% BF addition amount of BF-HA-composite emulsion-based cement were investigated respectively. The cement stone was sampled, and the phase of the corroded layer and the uncorroded layer was analyzed by XRD. The specific evaluation results are shown in Figure 13.

From Figure 13, the main phase of the 10% BF-HA-composite emulsion cement emulsion is calcite, and the main phases in the 0% BF-HA-composite emulsion cement emulsion

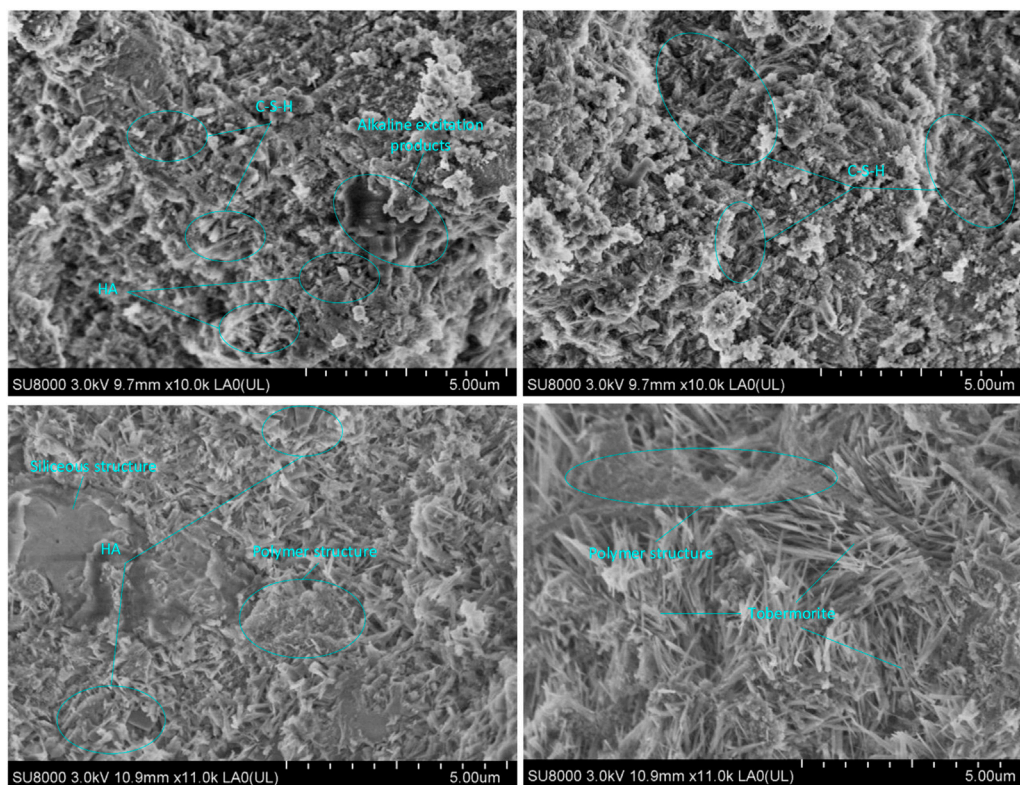


FIGURE 16

Microstructure of non-corrosive zone of BFs-HA-composite emulsion base cement paste.

are calcite and aragonite. In the 10% BFs-HA-composite emulsion base, the emulsion of hardened cement paste mainly contains calcareous stone,  $C_2S$ , C-S-H and a small amount of Tilleyite. In the 0% BFs-HA-composite emulsion base, the main corrosion layer is Hardstone and  $C_2S$ . This indicates that there is still emulsion silicate without high temperature conversion under the 28 days corrosion protection of BFs-HA-composite emulsion cement paste. The addition of BFs prolongs the hydration process of cement paste, and the sealing effect of primary pore of cement paste is continuing.

To explore the phase change of high density BFs-HA-composite emulsion cement paste under ultra-high temperature corrosion, the emulsion of emulsion 28 days and  $2.1 \text{ g/cm}^3$  BFs-HA-composite emulsion base cement samples were selected. XRD analysis of the sample fragments before and after corrosion was carried out. The specific evaluation results are shown in Figure 14.

It can be seen from Figure 14 that in the high-density BFs-HA-composite emulsion-based cement stone corrosion layer, the phases are calcite, aragonite, weighting agent and a small number of siliceous components; in the uncorroded area, the phases are weighting agent, silicon quality components, a small amount of grainy tobermorite and orthorhombic zeolite. Because of the high

proportion of iron ore powder in high density BFs-HA-composite emulsion cement, the characteristic peak is also obvious. In addition, by comparing with Figure 13, the residual phase in the high density BFs-HA-composite emulsion cement emulsion is basically consistent with the conventional density BFs-HA-composite emulsion cement except the weighting agent.

### 3.6.4 Micromorphology analysis before and after corrosion

To analyze the influence of the corrosion performance of the composite emulsion-based cement stone under the combination of BFs and HA, scanning electron microscopy was used to observe the section of the BFs-HA-composite emulsion-based cement stone when it was corroded for 28 days. Differences in microstructure between corroded and uncorroded layers of composite emulsion-based cement stone. The observation results of the BFs-HA-composite emulsion-based cement stone corrosion layer is shown in Figure 15.

From Figure 15, there is a small amount of scattered  $\text{CaCO}_3$  crystalline phase in the BFs-HA-composite emulsion-based cement stone corrosion layer, most of the  $\text{CaCO}_3$  crystalline phase exists in the form of aggregates, and a small amount of

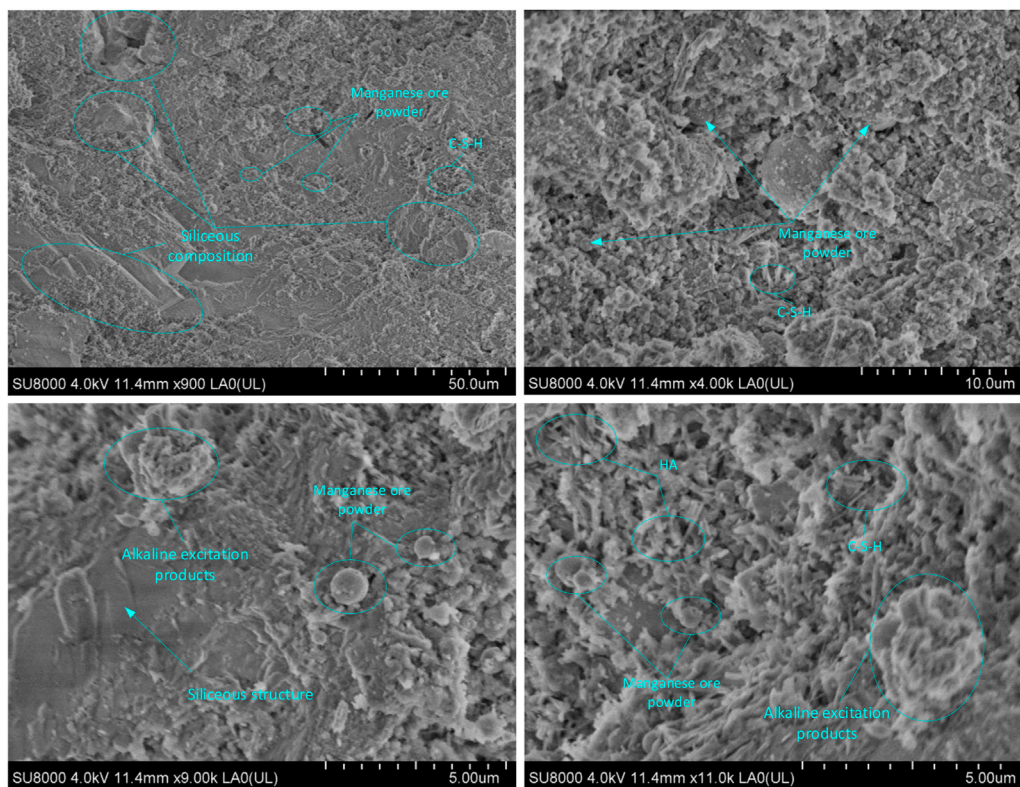


**FIGURE 17**  
Microstructure of non-corrosive zone of high density BF-HA-composite emulsion base cement paste.

polymer coating layer can be seen, no hard calcium silicate is seen. Stone,  $\text{Ca}(\text{OH})_2$ , and the profile shows good structural integrity. This is because in the BF-HA-composite emulsion-based cement stone, BF stimulates the relative hydration products to cement and fill the original pore structure, which effectively improves the compactness of the cement stone matrix, expands the coverage of the cement, and can also be used during the corrosion process. Cooperate with HA and polymer to further improve the structural integrity of the cross section.

The microstructure of the uncorroded area inside the BF-HA-composite emulsion-based cement stone is shown in Figure 16.

It can be seen from Figure 16 that the uncorroded area of the BF-HA-composite emulsion-based cement stone contains a large amount of alkali-excited minerals with high structural integrity, and a large amount of acicular tobermorite and a small amount of long flaky HA can be seen. Compared with the HA-composite emulsion-based cement stone, the matrix filler in the cross-section of the BF-HA-composite emulsion-based cement stone sample has a larger coverage area, higher integrity and density, thereby improving the intrusion of acidic corrosive media. Difficulty.

To find out the reasons why the weighting agent affects the corrosion performance of BF-HA-composite emulsion-based cement stone, the experimental samples with the same conditions as the XRD test were selected for scanning electron microscope observation, and the corrosion layer of high-density BF-HA-composite emulsion-based cement stone was analyzed. Differences in microstructure from that of the unetched layer. The experimental results are shown in Figures 17, 18.

According to Figures 17, 18, the main structure of silicon and a little globular manganese ore weighting agent can be found in the corrosion and non-corrosion section of high density BF-HA-composite emulsion. The non-corroded area is rich in a large amount of hydration products with rough boundary and slag excitation phase, but the cementation between hydration products is reduced and there are a certain number of micropores. The hydration products in the corrosion area show rounded edges and corners after dissolution, and there are obvious pore structures. This is because the addition of weighting agent indirectly reduces the free water in the cement slurry system, resulting in the reduction of the hydration degree of cement particles and the generation of BF excitation products, thus reducing the filling and

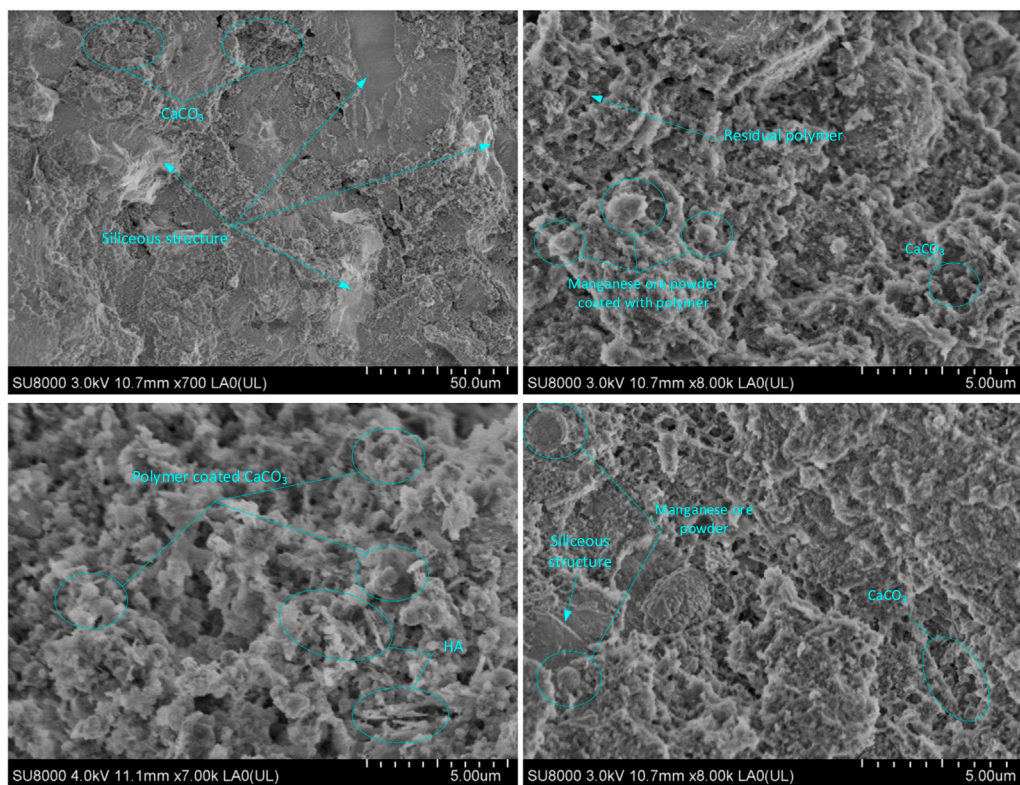


FIGURE 18

Microstructure of corrosion zone of cement paste with high density BFs-HA-composite emulsion.

cementation of microporous channels and reducing the corrosion performance of cement slurry.

## 4 Conclusion

Through the combination design and dosage optimization of anti-corrosion materials, a multicomponent composite ultra-high temperature anti-corrosion cement slurry system with different density was constructed, and the engineering and corrosion properties of the system at ultra-high temperature were studied. In addition, the microstructure and phase composition of cement paste are analyzed by combining various characterization methods. The experimental results are as follows:

1) In the high-temperature performance degradation experiment of cementing cement stone: the lower the number of silica fume, the larger the permeability pore between its particles, resulting in the gradual increase of water loss of cementing cement slurry and the gradual decrease of compressive strength. By controlling the silica fume ratio of high and low mesh number (325:800) at about 7:3, it

can ensure that the cementing cement slurry can obtain better slurry performance.

- 2) According to the engineering performance evaluation results of multi-component composite ultra-high temperature anti-corrosion cement slurry system with different densities, the system can maintain good slurry stability at 220°C and the thickening time is more than 5 h. In addition, under different densities, the *SPN* value is below 3, the pressure stability coefficient is greater than 1, and the conversion time from 48 Pa to 240 Pa is less than 15 min. The early strength of cement stone develops rapidly, and the compressive strength within 12 h can reach more than 20 MPa.
- 3) Through the study on the corrosion resistance of multi component composite ultra-high temperature corrosion resistant cement paste, it is known that with the increase of alkali activated BFs dosage, the initial compressive strength of cement paste increases gradually, the decline rate of compressive strength decreases, and the corrosion rate decreases regularly. And the anti-corrosion effect of HA and composite emulsion admixture will not be weakened.



- 4) Through the research on the corrosion performance of multicomponent composite ultra-high temperature corrosion resistant cement paste with different density, with the density of cement slurry system exceeding 2.1 g/cm<sup>3</sup>, the corrosion resistance of cement paste gradually weakens, the change value of permeability and the decline rate of compressive strength gradually increase, but it can still maintain a good corrosion prevention effect.
- 5) The high proportion of powder anti-corrosion admixture (BFs, HA) effectively solves the strength decline and high-temperature stability of cement stone under ultra-high temperature, and the pozzolanic effect and large pore filling effect effectively improve the compactness of cement stone. On the one hand, the multi-component composite lotion reduces the permeability of cement paste through curing film formation and microporous channel filling; on the other hand, the multi-component composite lotion improves its high-temperature stability and initial performance by reducing the filtration of cement slurry, thus increasing the difficulty of penetration of corrosive media. Erik, 1990, Lecourtier and Cartalos, 1993, Liu, 2001, Ramadan et al., 2019.

## Data availability statement

The original contributions presented in the study are included in the article/supplementary materials, further inquiries can be directed to the corresponding author.

## References

- Erik, B. (1990). *Nelson. Well cementing[M]*. Sugar Land, Texas: Schlumberger Dowell. Available at: <https://catalog.libraries.psu.edu/catalog/1974448>.
- Krivenko, P., Petropavlovskiy, O., and Kovalchuk, O. (2020). "Enhancement of alkali-activated slag cement concretes crack resistance for mitigation of steel reinforcement corrosion[C]," in *E3S web of conferences* (Kryvyi Rih, Ukraine: EDP Sciences).
- Kwatia, G., Ramadan, M., and Salehi, S. (2019). "Enhanced cement composition for preventing annular gas migration[C]," in *ASME 38th international conference on ocean* (Glasgow, Scotland, United Kingdom: Offshore and Arctic Engineering).
- Lecourtier, J., and Cartalos, U. (1993). *Cementing technology and procedures[M]*. Paris, France: Editions Technip.
- Liu, C. (2001). *Theory and application of cementing in oil and gas wells [M]*. Beijing, China: Petroleum Industry Press.
- Moore, L. P., Jones, J. E., and Perlman, S. H. (2012). "Evaluation of precompletion annular gas leaks in a Marcellus lateral[C]," in *SPE americas unconventional resources conference*.
- Ramadan, M., Salehi, S., and Kwatia, G. (2019). Experimental investigation of well integrity: Annular gas migration in cement column[J]. *J. Petroleum Sci. Eng.* 179 (8), 126–135.
- Rogers, M. J., Dillenbeck, R. L., and Eid, R. N. (2004). "Transition time of cement slurries, definitions and misconceptions, related to annular fluid migration[C]," in *SPE annual technical conference and exhibition* (Houston, Texas: Society of Petroleum Engineers).
- Rooby, D. R., Kumar, T. N., Harilal, M., Sofia, S., George, R., and Philip, J. (2021). Enhanced corrosion protection of reinforcement steel with nanomaterial incorporated fly ash based cementitious coating. *Constr. Build. Mater.* 275 (3), 122130–122216. doi:10.1016/j.conbuildmat.2020.122130
- Sutton, D. L., Paul, R., and Sabins, F. (1984). New evaluation for annular gas-flow potential[J]. *Oil Gas J.* 82 (51), 1–9.
- Wang, Y., Chen, Y. F., Lu, Y., Zhang, H. F., and Sun, Z. G. (2012). Compressive strength changing law of oil well cement paste under corporate corrosion of HCO<sub>3</sub><sup>-</sup> and SO<sub>4</sub><sup>2-</sup> [J]. *Appl. Mech. Mater.* 229-231 (11), 95–99. doi:10.4028/www.scientific.net/amm.229-231.95
- Xu, B., Yuan, B., and Wang, Y. (2018). Anti-corrosion cement for sour gas (H<sub>2</sub>S-CO<sub>2</sub>) storage and production of HTHP deep wells[J]. *Appl. Geochem.* 96, 155–163.
- Xue, Z., He, D., and Wang, X. (2013). Methods study on gas channeling of *in situ* combustion development in developed heavy oil reservoir. *Appl. Mech. Mater.* 316 (4), 834–837. doi:10.4028/www.scientific.net/amm.316-317.834
- Yuan, B., Wang, Y., Yang, Y., Xie, Y., and Li, Y. (2018). Wellbore sealing integrity of nanosilica-latex modified cement in natural gas reservoirs with high H<sub>2</sub>S contents[J]. *Constr. Build. Mater.* 192, 621–632. doi:10.1016/j.conbuildmat.2018.10.165
- Zhang, B., Zou, C., Peng, Z., Zheng, Y., and Zhang, J. (2020). Study on the preparation and anti-CO<sub>2</sub> corrosion performance of soap-free latex for oil well cement[J]. *ACS omega* 5 (36), 23028–23038. doi:10.1021/acsomega.0c02729
- Zhang, J., Liu, K., and Hou, R. (2014). *Development and change of compressive strength for class g oil well cement under high temperature[C]*//*Advanced Materials Research*. Switzerland, Europe: Trans Tech Publications Ltd.
- Zhang, Y., Xu, M., Song, J., Wang, C., Wang, X., and Hamad, B. A. (2022). Study on the corrosion change law and prediction model of cement stone in oil wells with CO<sub>2</sub> corrosion in ultra-high-temperature acid gas wells[J]. *Constr. Build. Mater.* 323 (3), 125879–125914. doi:10.1016/j.conbuildmat.2021.125879
- Zuo, J., Li, H., Dong, B., and Wang, L. (2020). Effects of metakaolin on the mechanical and anticorrosion properties of epoxy emulsion cement mortar. *Appl. Clay Sci.* 186 (3), 105431–105513. doi:10.1016/j.clay.2019.105431

## Author contributions

YZ investigated and processed the data, pointed out the framework of the paper, made a summary and analysis, and completed the writing of the article. YZ reviewed the paper and supported the project. YH reviewed and corrected the article.

## Funding

This work was supported by The Doctoral Fund Project of Chongqing Institute of Industry and Technology (Grant No. 2022G2YBS2K2-12).

## Conflict of interest

The author declares that the research was conducted in the absence of any commercial or financial relationships that could be construed as a potential conflict of interest.

## Publisher's note

All claims expressed in this article are solely those of the authors and do not necessarily represent those of their affiliated organizations, or those of the publisher, the editors and the reviewers. Any product that may be evaluated in this article, or claim that may be made by its manufacturer, is not guaranteed or endorsed by the publisher.